University of Groningen

Identification of Variants in RET and IHH Pathway Members in a Large Family With History of Hirschsprung Disease

Sribudiani, Yunia; Chauhan, Rajendra K.; Alves, Maria M.; Petrova, Lucy; Brosens, Erwin; Harrison, Colin; Wabbersen, Tara; de Graaf, Bianca M.; Rugenbrink, Tim; Burzynski, Grzegorz

IMPORTANT NOTE: You are advised to consult the publisher's version (publisher's PDF) if you wish to cite from it. Please check the document version below.

Document Version
Publisher's PDF, also known as Version of record

Link to publication in University of Groningen/UMCG research database

BASIC AND TRANSLATIONAL—ALIMENTARY TRACT

Identification of Variants in RET and IHH Pathway Members in a Large Family With History of Hirschsprung Disease

Yunia Sribudiani,[1,2,*] **Rajendra K. Chauhan**,[1,*] **Maria M. Alves**,[1,*] Lucy Petrova,[3] Erwin Brosens,[1] Colin Harrison,[3] Tara Wabbersen,[3] Bianca M. de Graaf,[1] Tim Rügenbrink,[1] Grzegorz Burzynski,[3] Rutger W. W. Brouwer,[4] Wilfred F. J. van IJcken,[4] Saskia M. Maas,[5] Annelies de Klein,[1] Jan Osinga,[6] Bart J. L. Eggen,[7] Alan J. Burns,[1,8] Alice S. Brooks,[1] Iain T. Shepherd,[3] and Robert M. W. Hofstra[1,8]

[1]Department of Clinical Genetics, and [4]Erasmus Center for Biomics, Erasmus Medical Center, Rotterdam, The Netherlands; [2]Department of Biomedical Sciences, Division of Biochemistry and Molecular Biology, Faculty of Medicine, Universitas Padjadjaran, Bandung, Indonesia; [3]Department of Biology, Emory University, Atlanta, Georgia; [5]Department of Clinical Genetics, Academic Medical Center, University of Amsterdam, Amsterdam, The Netherlands; [6]Department of Genetics, and [7]Department of Neuroscience, Section Medical Physiology, University Medical Center Groningen, University of Groningen, Groningen, The Netherlands; and [8]Neural Development and Gastroenterology Units, UCL Institute of Child Health, London, UK

BACKGROUND & AIMS: Hirschsprung disease (HSCR) is an inherited congenital disorder characterized by absence of enteric ganglia in the distal part of the gut. Variants in ret proto-oncogene (RET) have been associated with up to 50% of familial and 35% of sporadic cases. We searched for variants that affect disease risk in a large, multigenerational family with history of HSCR in a linkage region previously associated with the disease (4q31.3–q32.3) and exome wide. **METHODS:** We performed exome sequencing analyses of a family in the Netherlands with 5 members diagnosed with HSCR and 2 members diagnosed with functional constipation. We initially focused on variants in genes located in 4q31.3–q32.3; however, we also performed an exome-wide analysis in which known HSCR or HSCR-associated gene variants predicted to be deleterious were prioritized for further analysis. Candidate genes were expressed in HEK293, COS-7, and Neuro-2a cells and analyzed by luciferase and immunoblot assays. Morpholinos were designed to target exons of candidate genes and injected into 1-cell stage zebrafish embryos. Embryos were allowed to develop and stained for enteric neurons. **RESULTS:** Within the linkage region, we identified 1 putative splice variant in the lipopolysaccharide responsive beige-like anchor protein gene (LRBA). Functional assays could not confirm its predicted effect on messenger RNA splicing or on expression of the mab-21 like 2 gene (MAB21L2), which is embedded in LRBA. Zebrafish that developed following injection of the lrba morpholino had a shortened body axis and subtle gut morphological defects, but no significant reduction in number of enteric neurons compared with controls. Outside the linkage region, members of 1 branch of the family carried a previously unidentified RET variant or an in-frame deletion in the glial cell line derived neurotrophic factor gene (GDNF), which encodes a ligand of RET. This deletion was located 6 base pairs before the last codon. We also found variants in the Indian hedgehog gene (IHH) and its mediator, the transcription factor GLI family zinc finger 3 (GLI3). When expressed in cells, the RET-P399L variant disrupted protein glycosylation and had altered phosphorylation following activation by GDNF. The deletion in GDNF prevented secretion of its gene product, reducing RET activation, and the IHH-Q51K variant reduced expression of the transcription factor GLI1. Injection of morpholinos that target ihh reduced the number of enteric neurons to 13% ± 1.4% of control zebrafish. **CONCLUSIONS:** In a study of a large family with history of HSCR, we identified variants in LRBA, RET, the gene encoding the RET ligand (GDNF), IHH, and a gene encoding a mediator of IHH signaling (GLI3). These variants altered functions of the gene products when expressed in cells and knockout of ihh reduced the number of enteric neurons in the zebrafish gut.

Hirschsprung disease (HSCR) is a congenital disorder characterized by the absence of enteric ganglia in variable lengths of the distal gut. As a consequence, functional networks of neurons and glia, the intrinsic innervations of the gastrointestinal tract comprising the enteric nervous system (ENS), cannot be established,[1] leading to intestinal obstruction by dysregulated smooth muscle contraction/relaxation.

HSCR is considered to be an inherited disease. This assumption is based on several lines of evidence, including familial occurrence (∼5%), elevated risk of occurrence in

---

*Authors share co-first authorship.

Ⓜ Most current article

WHAT YOU NEED TO KNOW

BACKGROUND AND CONTEXT

Hirschsprung disease (HSCR) arises due to failure of the enteric neurons to colonize the gut. It is an inherited disorder, but the genetic cause is unknown in the majority of cases.

NEW FINDINGS

In a Dutch multigenerational family with history of HSCR, the authors identified variants in *RET*, *GDNF*, *IHH* and *GLI3* that disrupt the function of their encoded proteins, contributing to disease development.

LIMITATIONS

The variants identified in this family are rare and unlikely to explain the missing heritability seen in the majority of HSCR cases.

IMPACT

This study confirms *RET* as the major HSCR gene and shows that a combination of rare variants in *GDNF*, *IHH* and *GLI3*, modulates clinical expression of the disease phenotype.

---

siblings (relative risk as high as 200), association with chromosomal abnormalities, and the existence of many naturally occurring animal models with colonic aganglionosis.[2] The mode of inheritance can vary from dominant with reduced penetrance, mostly found in nonsyndromic familial HSCR cases, to recessive, in families with syndromic HSCR.[2] Sporadic HSCR cases also have been reported and are believed to be multifactorial and polygenic in nature, suggesting the involvement of several genes in concert.

The search for genes involved in HSCR has been extensive and ranged from classical linkage to genome-wide association studies and candidate gene approaches. To date, mutations in approximately 20 genes have been identified.[3–5] However, the REarranged during Transfection (*RET)* gene is still considered to be the major HSCR gene, as 50% of familial cases and 15% to 35% of sporadic cases carry a mutation in its coding or messenger RNA (mRNA) splicing regions. The *RET* locus (10q11) was the first one to be identified for HSCR,[6] and, subsequently, coding variants in this gene were reported to give rise to a dominant form of the disease with incomplete penetrance (72% for male and 51% for female individuals).[7–10] Moreover, all association studies conducted on sporadic HSCR cases showed the highest association with a low-penetrant variant present in intron 1 of *RET* (odds ratio = 2 when heterozygous and odds ratio = 20 when homozygous).[11,12] Taken together, these genetic findings showed that *RET* variants can be high- or low-penetrant, but more importantly, they demonstrated that almost every patients with HSCR has a variant in *RET*. Thus, *RET* seems to be crucial in developing HSCR, but it is also likely that one or more modifier genes, as well as environmental factors, are involved in disease pathogenesis, even when a high penetrant *RET* mutation is found.[13,14] Linkage analysis conducted on 12 multiplex HSCR families

corroborated this idea. Although 11 families showed linkage to the *RET* locus, only half of them (6) carried a severe *RET* coding mutation.[14] Intriguingly, the remaining 5 families also showed linkage to 9q31, suggesting the involvement of a modifier gene at this locus.[15] After these early findings, subsequent studies were conducted to search for modifier loci in HSCR. Sib-pair analysis resulted in the identification of 2 additional loci at 3p21 and 19q12,[16] haplotype sharing in a large Mennonite kindred identified a new locus on 16q23,[17] linkage analysis in a multigenerational Dutch family identified a locus at 4q31.3-q32.3,[18] and genome-wide association studies also have identified loci at 7q21.11 and 8p12.[5,19] However, combinations of distinct rare mutations resulting in HSCR are not frequently reported.[4,20–22]

In this article, we focus on one family in which a 12.2-Mb interval suggestive for linkage was identified on 4q31.3-q32.3 (chr4: 142,197,646–158,353,484 [Hg19]), but no pathogenic variants in the known HSCR genes have been found.[18] Based on the pedigree, incomplete penetrance of a disease-associated variant was expected, suggesting the involvement of several genes. In an attempt to identify the genetic cause of HSCR in this family, we have now used whole-exome sequencing to search for yet unidentified pathogenic rare variants or modifier genes. We determined segregation patterns for candidate variants, and performed in vitro and in vivo studies to test the involvement of the identified candidate genes in disease pathogenesis, revealing the complex genetic nature of HSCR.

Materials and Methods

Patient Information

A multigenerational Dutch family was included in this study. This family is composed of 5 individuals diagnosed with HSCR (IV-3, V-1, V-2, V-3, and V-4), and 2 diagnosed with functional constipation (III-1 and IV-2) (Figure 1). A detailed description of the phenotypes has been previously reported.[18] Written informed consent was obtained from the parents for diagnostic analysis.

Exome Sequencing and Variant Prioritization

Two HSCR-affected individuals (V-1 and V-4) from different branches of the family were initially selected for exome sequencing. In a later stage of the study, IV-4 and IV-5 were also included (Figure 1). Three micrograms of DNA from each of the individuals was used. Details about execution and data analysis can be found in supplementary data.

Validation of Candidate Variants and Family Screening

Genomic DNA was isolated from peripheral blood leucocytes using a standard protocol previously described.[23] Candidate variants were validated by Sanger sequencing as previously described.[24] Segregation analysis was performed using family members for which DNA was available (II-2, III-2, IV-1, IV-2, IV-3, IV-4, IV-5, V-1, V-2, V-3, and V-4).
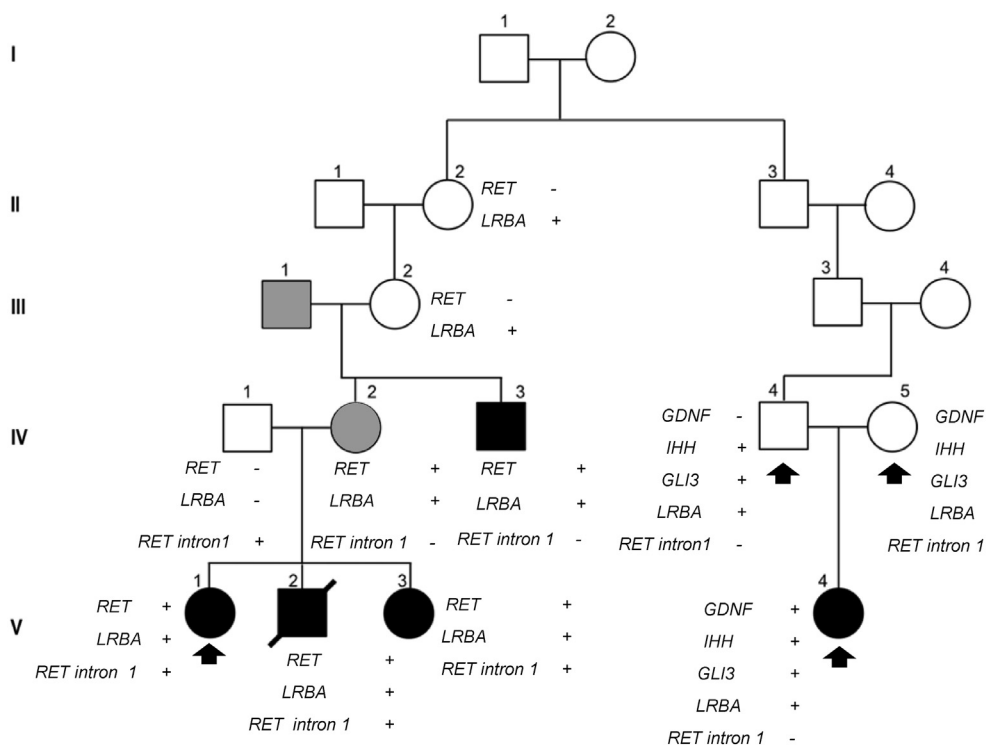
Figure 1. Pedigree of the multigenerational Dutch family. Subjects affected with HSCR are represented as *black symbols* (IV-3, V-1, V-2, V-3, and V-4), and those affected with constipation are marked in *gray* (III-1 and IV-2). Individuals submitted to whole-exome sequencing are marked with *arrows*. Segregation analysis was performed, and the presence (+) or absence (−) of variants located in the identified candidate genes is also represented.

Vector Design and Site Direct Mutagenesis

Vectors used are described in detail in supplementary data.

Whole-Mount In Situ Hybridization for lrba, mab21l2, and ihh in Zebrafish

lrba (lipopolysaccharide responsive beige-like anchor), *mab21l2* (Mab-21-Like 2), and *ihh* (Indian hedgehog) genes were amplified from total mRNA collected from zebrafish embryos at 48 hours post fertilization (hpf), by reverse transcription polymerase chain reaction (RT-PCR) using a One-Step RT-PCR Kit (Qiagen, Valencia, CA). Primers used are described in Supplementary Table 1. A detailed protocol can be found in supplementary data.

lrba, mab21l2, and ihh Morphant Analysis in Zebrafish

Two splice blocking morpholinos were designed to target exon 13 (AGTTGGTTTAGTCTCTTACCGAGAC) and exon 24 (ACTGCATACTAACCGAAGAAGAAGT) of *lrba*. The effectiveness of these morpholinos was confirmed by RT-PCR. A previously described translation blocking morpholino for *mab21l2* (ACTGTAGACCGGAGTTTCGCAGTAC) was used[25] (Gene Tools, Philomath, OR). A *mab21l2* mutant line (au12 allele) was also analyzed.[26] The *ihh* morpholino (GGAGACGCATTCCACCGCA AGCG) was designed to target the transcription start site of *ihh*, as previously described.[27] Morphants were generated by injecting 100 μM of each morpholino into 1-cell-stage zebrafish embryos. Morphant/mutant and control embryos were allowed to develop until 120 hpf and were fixed and stained for ENS neurons using the HuC/D antibody (Invitrogen, Carlsbad, CA), as previously reported.[28] A *p53* control morpholino (Gene Tools) was coinjected in all morphant and control embryos, to suppress apoptotic effects induced as a secondary effect of the morpholinos, as described elsewhere.[29] To determine the number of enteric neurons present, a 10-segment length of the gut to the vent was counted. The numbers in the text represent percent of control ± SEM for at least 5 separate embryos per morpholino/mutant genotype. Significance was determined by the Student t test with significance assessed when $P < .0005$.

Cell Culture and Transfections

Human embryonic kidney (HEK293) cells, COS-7 cells (CV-1 [simian] in origin, and carrying the SV40 genetic material), and control fibroblasts were cultured in Dulbecco's modified Eagle's minimal essential medium (GIBCO, Waltham, MA) containing 10% fetal bovine serum (GIBCO) and penicillin/streptomycin (GIBCO). The neuroblastoma cell line (Neuro-2a) (CCL-131; American Type Culture Collection, Manassas, VA) was cultured according to the protocol of the American Type Culture Collection. All cell lines were incubated at 37°C, and supplied with 5% CO_2. Transfection was performed as described before.[30]

Exon Trap Assays

The exon trap assays were performed as described before.[31,32] SD6 and SA2 primers are described in Supplementary Table 1.

Luciferase Assays

Neuro-2a cells were transfected with 1 μg of SV40-P or LRBA-wild-type (WT)/mutant (Mut) vectors and cotransfected with 10 ng of internal control, pRL-SV40-Renilla Luciferase (Promega, Madison, WI). Luciferase activity was measured and

quantified as described before.[33] SV40-E (without any promoter) was used as a negative control and RET-WT-enhancer was used as a positive control.[33] Luciferase assays were performed in 3 independent, triplicate experiments (n = 9).

Activation of the Indian Hedgehog Signaling

HEK293 cells cultured in a 6-well plate were transiently transfected with pCMV-IHH-FLAG-WT/Mut. After 24 hours, the medium of transfected cells (conditioned medium) was collected and filtered using a 0.45-μm filter; 200,000 to 300,000 control human fibroblast cells were cultured in a 6-well plate for 24 hours. After this period, the medium was replaced by 1 mL fresh complete medium and 500 μL conditioned medium (containing secreted IHH-WT or IHH-Mut). Conditioned medium derived from nontransfected HEK293 cells was used as a negative control. Medium supplemented with 20 μM Purmophamine (Calbiochem, San Diego, CA) was used as a positive control for activation of the Hedgehog (Hh) signaling; 500 μL conditioned medium was concentrated using an M-10 filter (Millipore, Bedford, MA) and used for Western blot to determine the levels of IHH-WT and IHH-Mut protein secreted into the medium.

Glial Cell–Derived Neurotrophic Factor Stimulation and Western Blot

HEK293 cells were transiently cotransfected with pCMV-RET-WT/Mut (P399L), pCMV-GFRα1, and pNE–green fluorescent protein (GFP). After 24 hours, cells were treated with 50 ng/mL glial cell–derived neurotrophic factor (GDNF) (PeproTech EC, London, UK) for 15 minutes. To test the effect of the GDNF deletion, conditioned medium collected from HEK293 cells transfected with a GDNF-WT or GDNF-Mut constructs was collected in a similar way as described for IHH, and used to stimulate HEK293 cells transfected with pCMV-RET-WT, pCMV-GFRα1, and pNE-GFP. An amount of 500 μL of conditioned medium was also concentrated as described for IHH, and used to determine the levels of GDNF-WT and GDNF-Mut protein secreted into the medium by Western blot. Cell lysis, protein quantification, and Western blot were performed as previously described.[30] Primary and secondary antibodies used are described in Supplementary Table 2.

RNA Isolation and qReal-time-PCR

RNA isolation, complementary DNA preparation, and quantitative real-time (qRT) PCR are described in supplementary data.

Statistical Analysis

All results are expressed as the mean ± standard deviation or standard error of the mean. All data were analyzed using a 2-tailed Student t test or the χ^2 test. $P < .05$ was considered to be statistically significant.

Results

A Putative Splice Variant in LRBA Was Found in the Linkage Interval

Exome sequencing data collected from patients V-1 and V-4 were first analyzed to detect variants present in the linkage interval previously identified.[18] Exons that were not totally covered within this region (7 exons), were Sanger sequenced. From the exome analysis, only 1 rare variant (Exome Aggregation Consortium: 0.002534, and Genome of the Netherlands database: 0.009), predicted to be deleterious was found: a putative splice variant affecting exon 20 of the LRBA gene (NM_001199282.2:c.2444A>G) (Table 1 and Supplementary Table 3). LRBA was also found to be expressed in mouse gut,[34] leading us to consider it the best candidate gene for this family. Sanger sequencing confirmed the presence of the LRBA variant in all family members for which DNA was available (n = 11), and segregation patterns were determined (Figure 1; Supplementary Table 4).

Irba Is Not Required for ENS Development in Zebrafish

To investigate a possible role for LRBA in ENS development, we used the zebrafish as a model system. A single zebrafish ortholog for lrba was identified in an Ensemble gene search, which showed strong sequence similarity, as well as genome organization, to its human ortholog (82% homology). Whole-mount in situ hybridization revealed that lrba has a comparatively restricted expression pattern in zebrafish (Figure 2A). At 24 hpf, lrba expression was identified along the yolk sac boundary and weakly in the hindbrain. At 48 hpf, lrba was still weakly present in the hindbrain, and no apparent expression was detected elsewhere in the embryo (Figure 2A). A similar pattern of expression was detected at 72 and 96 hpf. However, at 72 hpf, lrba expression appeared in the intestinal bulb, and it was maintained at 96 hpf (Figure 2A). We also designed 2 different splice blocking morpholinos to suppress expression of this gene in zebrafish. Examination of lrba morphants at 120 hpf revealed a shortened body axis and subtle gut morphological defects. However, no significant reduction in the number of enteric neurons was detected when compared with controls, as the number of neurons in lrba morphants was 97.2% ± 4.8% of control (n = 17; Figure 2B).

Lack of Splicing Effect and Enhancing Defects for the LRBA Variant

The LRBA variant identified in this family (NM_001199282.2:c.2444A>G) is predicted to affect mRNA splicing of exon 20 by 1 of the 5 splice site prediction programs included in the Alamut splicing prediction module (http://www.interactive-biosoftware.com/alamut-visual/). To confirm pathogenicity of this variant, exon trap assays were performed, but no splice defect was detected. Similar-size bands of spliced product were observed in both the WT and Mut situations (Figure 3A).

Within intron 42 of LRBA, another gene called Mab-21-Like 2 (MAB21L2) is found (Figure 3B). A previous study has shown that expression of MAB21L2 can be controlled in a tissue-specific manner by several enhancer elements present within LRBA.[35] This led us to hypothesize that exon 20 of LRBA might work as one of these enhancers, and that the variant identified in this gene might disturb expression of MAB21L2. Because the role of MAB21L2 in ENS

Table 1. Rare variants identified in patients V-1 (a) and/or V-4 (b)

Sample	Gene	HGVS cDNA	Location	Effect	Exon	HGVS protein	dbSNP	Inherited from	ExAC MAF	GoNLMAF	Linkage region	HSCR gene panel	ClinVar
a	RET	NM_020975.4:c.1196C>T	E	MS	6	p.Pro399Leu	-	M	0	0	No	Yes	SCV000328919
a, b	NRP2	NM_201266.1:c.1000C>T	E	MS	7	p.Arg334Cys	rs114144673	F	0.0015737	0.006	No	No	SCV000328912
a, b	PGRMC2	NM_006320.4:c.185G>A	E	MS	1	p.Gly62Glu	rs41298555	F	0.0003475	0	No	No	SCV000328913
a, b	LRBA	NM_001199282.2:c.2444A>G	E	MS, PSE	20	p.Asn815Ser	rs140666848	M; F	0.0025336	0.018	Yes	No	SCV000328914
a, b	OR1F1	NM_012360.1:c.47G>A	E	MS	1	p.Gly16Glu	rs142486394	F	0.0026051	0.016	No	No	SCV000328915
a, b	CLUH	NM_015229.3:c.3547G>C	E	MS	24	p.Asp1183His	rs201361018	F	0.0001642	0	No	No	SCV000328921
a,b	PELP1	NM_014389.2:c.2696T>C	E	MS	16	p.Val899Ala	rs199636910	F	0.007134	0.009	No	No	-
a,b	PELP1	NM_014389.2:c.2161A>G	E	MS	16	p.Met721Val	rs200062536	F	0.001568	0.006	No	No	-
b	IHH	NM_002181.3:c.151C>A	E	MS	1	p.Gln51Lys	-	M	0	0	No	Yes	SCV000328908
b	GLI3	NM_000168.5:c.2119C>T	E	MS	14	p.Pro707Ser	rs121917716	F	0.0001976	0.002	No	Yes	SCV000328910
b	GDNF	NM_001190468.1:c.676_681delGGATGT	E	IFD	3	p.Gly226_Cys227del	-	DN	0	0	No	Yes	SCV000328917

NOTE. Build hg19, # public databases are 1000 Genomes, ESP6500, and Genome of the Netherlands (GoNL). All variants are heterozygous. The variants in *GL13* and *RET* are known deleterious variants.

cDNA, complementary DNA; dbSNP, Single Nucleotide Polymorphism database; DN, de novo; E, exon; ExAC, Exome Aggregation Consortium; F, Father; HGVS, Human Genome Variation Society; IFD, in-frame deletion; M, Mother; MAF, minor allele frequency; MS, missense; PSE, putative splice effect.

development is unknown, we first investigated the expression pattern of this gene in zebrafish, by performing whole-mount in situ hybridization at different stages of embryonic development. *mab21l2* was already known to be strongly expressed in the hindbrain and cranial neural crest in zebrafish.[25] Our results confirmed this expression pattern, and revealed strong expression of this gene in the pharyngeal arches, especially at 48 hpf (Supplementary Figure 1). We also observed a significant expression of *mab21l2* in the gut mesoderm from 48 hpf onward, which has not been reported before (Supplementary Figure 1). To investigate the importance of *MAB21L2* for ENS development, we initially used a morpholino-based approach to knock down this gene in zebrafish. Subsequently, we obtained a *mab21l2* mutant line (au12 allele).[26] Morphant and mutant fish had identical phenotypes with defects in development of pharyngeal arches and intestinal smooth muscle, as previously reported.[25] Critically, we detected a significant reduction in the number of enteric neurons in *mab21l2* homozygous mutants, which was 28.2% ± 3.8% of that seen in WT siblings (n = 12; Figure 3*C*). These results led us to conclude that *mab21l2* is required for ENS development in zebrafish, and that it might therefore also contribute to HSCR pathogenesis in humans. To further explore this possibility, we investigated whether the *LRBA* variant found in this family acts as a prospective enhancer element, thereby affecting *MAB21L2* expression. For this, a series of luciferase assays was performed using exon 20 of *LRBA* and its flanking regions, containing the WT or the Mut sequence (c.2444A>G). Our results showed that exon 20 of *LRBA* could indeed enhance the promoter activity of SV40 (Figure 3*D*). However, no difference was detected when the *LRBA* variant (c.2444A>G) was introduced (Figure 3*D*). Considering this result, we were unable to link *MAB21L2* to HSCR, as it is unlikely that the *LRBA* variant identified has an enhancing effect. However, to rule out the possibility that a mutation in *MAB21L2* was missed in the exome analysis, we Sanger sequenced all exons of *MAB21L2* and its regulatory regions (16 Kb upstream), in patients V-1 and V-4. No rare variants were identified that could be associated to the disease phenotype.

Variants in RET, IHH, GLI3, and GDNF Were Detected Outside the Linkage Interval

As we were unable to confirm pathogenicity of the variant found in *LRBA*, and could not find a link between *MAB21L2* and HSCR pathogenesis, we hypothesized that variants outside the linkage interval would be the ones determining disease development. Therefore, we focused on nonshared rare variants outside the linkage interval present in any of the 2 individuals sequenced (V-1 and V-4). A de novo analysis was also performed using the trio composed of IV-4, IV-5, and V-4. Initially, these 2 analyses aimed to find variants present in genes previously associated with HSCR.[3,4] Moreover, variants were prioritized based on function and deleteriousness. With this approach, we found a previously unidentified rare variant in *RET* (NM_020975.4:c.1196C>T; p.P399L) in patient V-1 (Table 1 and Supplementary Table 3). Segregation analysis showed
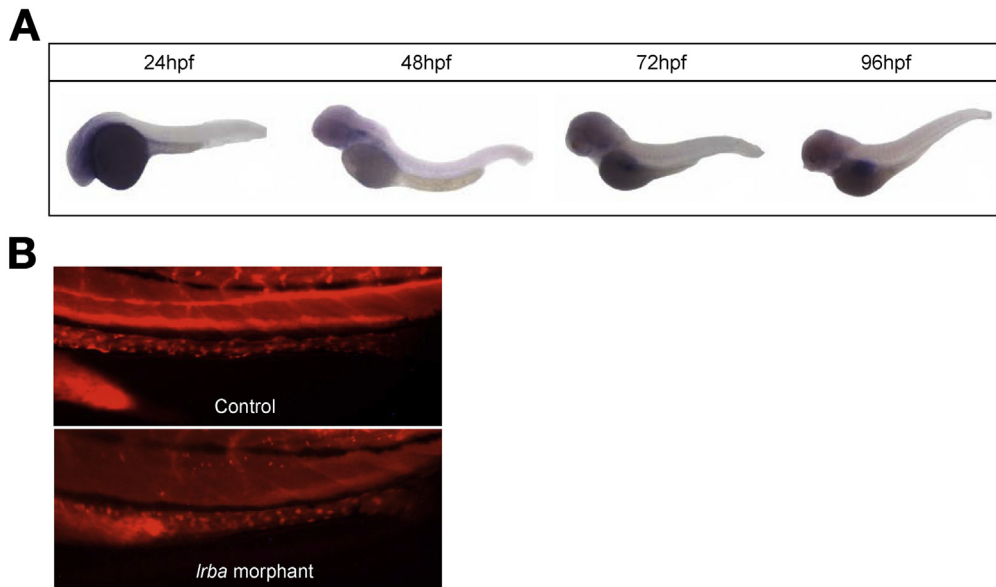
Figure 2. *Irba* is expressed in the gut but it is not required for ENS development in zebrafish. (*A*) In situ hybridization performed in zebrafish embryos showed the expression pattern of *Irba* during embryonic development. At 24 hpf, Irba is present along the yolk sack and is weakly expressed in the hindbrain. This pattern of expression is detected throughout all time points analyzed. From 72 hpf, a strong signal is detected in the intestinal bulb (*arrows*). (*B*) HuC/Elavl3 staining showed that the distribution and number of enteric neurons along the gut in *Irba* morphants is similar to controls.

that the 2 affected siblings of patient V-1 (V-2 and V-3), the unaffected mother (IV-2), and the affected maternal uncle (IV-3) also carry the same heterozygous *RET* variant, whereas the grandmother (III-2) does not (Figure 1, Supplementary Table 4). Due to DNA unavailability, we were unable to confirm the presence of this variant in the grandfather (III-1). However, considering that both the mother (IV-2) and the grandfather (III-1) were reported to suffer from severe constipation in childhood, and the grandmother (III-2) had no intestinal complains, it is likely that this *RET* variant was inherited from the grandfather (III-1). For patient V-4, 2 rare variants were identified in 2 different genes: Indian hedgehog (*IHH*) (NM_002181.3:c.151C>A; p.Q51K), and the GLI family zinc finger 3 (*GLI3*) (NM_000168.5:c.2119C>T; p.P707S) (Table 1 and Supplementary Table 3). Segregation analysis showed that both variants were inherited from the father (Figure 1, Supplementary Table 4). The de novo analysis performed for patient V-4 also identified a heterozygous in-frame deletion in the Glial cell–derived neurotrophic factor gene (*GDNF*) (NM_001190468.1:c.676_681delGGA TGT) (Figure 1, Table 1). No allelic frequencies of any of these variants were found in the available databases.

RET-P399L Disturbs Protein Glycosylation and Affects Phosphorylation on GDNF Activation In Vitro

To determine the effect of the *RET* rare variant identified in the first branch of the family (c.1196C>T, p.P399L), we examined the glycosylation and phosphorylation status of the mutant protein and compared it with the WT. As expected, 2 bands were identified in the presence of the RET-WT–expressing vector (Figure 4*A*). The lower band

(~150 kDa) corresponds to the unglycosylated RET protein, whereas the upper one (~170 kDa) is the glycosylated (mature) RET protein. In the presence of the RET-Mut (RET-P399L) expressing vector, only the lower band was detected, suggesting that this variant disturbs protein glycosylation (Figure 4*A*). RET phosphorylation was also investigated on GDNF stimulation, and in the presence of the Mut-expressing vector, RET phosphorylation was dramatically reduced (Figure 4*A*). These results confirm pathogenicity of the *RET* variant identified.

IHH-Q51K Disturbs Activation of Hedgehog Signaling In Vitro

To study the effect of the *IHH* variant identified in patient V-4 (c.151C>A, p.Q51K), we transiently transfected HEK293 cells with *IHH*-WT-FLAG and *IHH*-Q51K-FLAG vectors. Comparative expression levels of the precursor form of IHH-WT (~46 kDa) and IHH-Q51K were found in the cell lysates and in the conditioned medium from transfected HEK293 cells (Figure 4*B*). However, a significant lower expression of the transcriptional target of Hh signaling, *GLI1*, was identified by qreal time-PCR in fibroblasts cultured in the presence of conditioned medium containing the secreted form of mutant IHH (Figure 4*C*). This result confirms pathogenicity of the *IHH* variant identified.

ihh Is Required for ENS Development in Zebrafish

Transgenic zebrafish embryos *Tg(-8.3phox2b:Kaede)* were injected with a morpholino designed to specifically target expression of *ihh* to further study the involvement of this gene in ENS development. Morphant and uninjected control embryos were visualized at 120 hpf and several
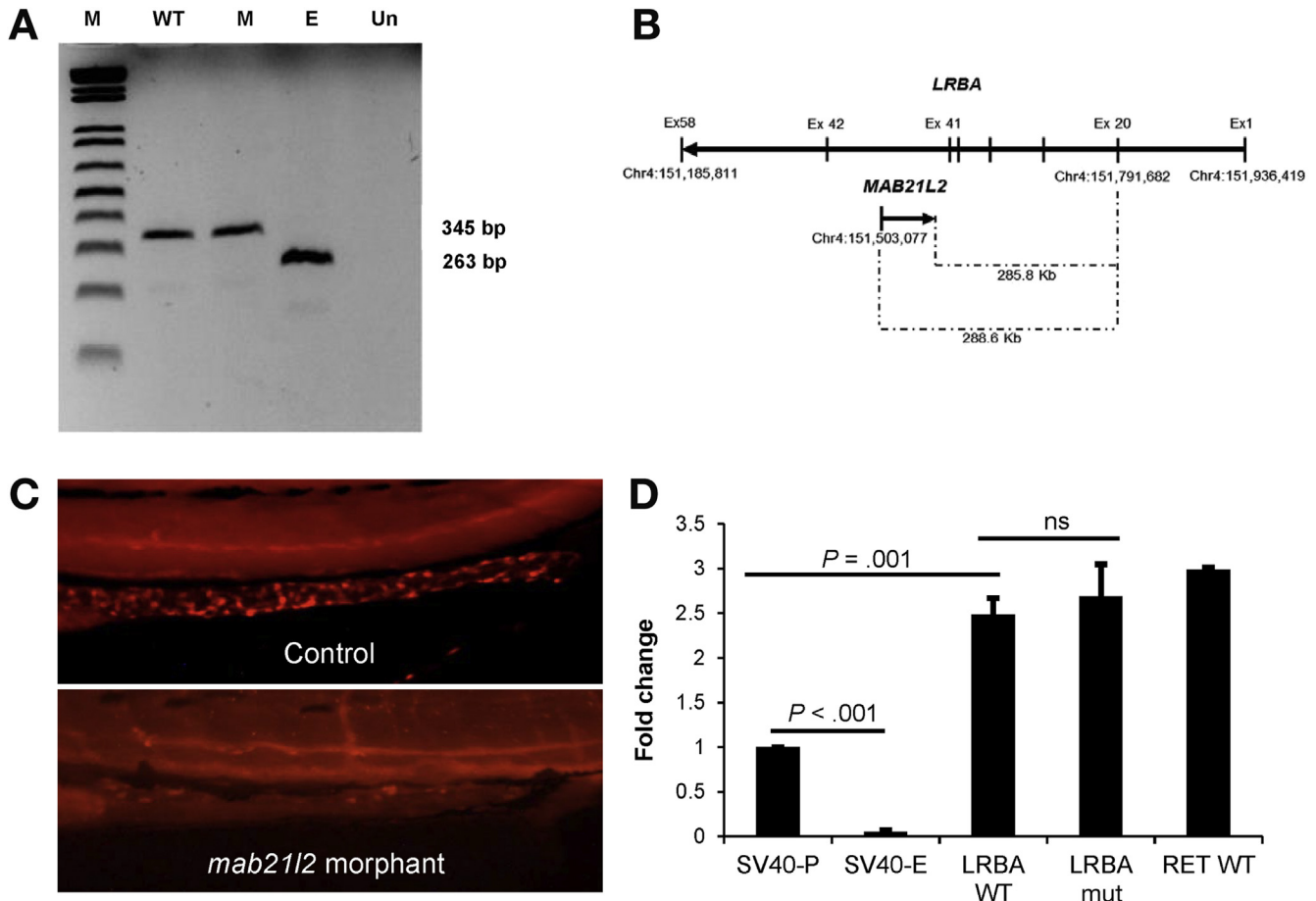
Figure 3. The *LRBA* variant identified does not affect splicing nor its enhancing ability, and is likely not involved in the regulation of *MAB21L2* expression. (*A*) Exon trap assay showed that splicing of exon 20 of *LRBA* is not affected by the presence of the variant identified (c.2444A>G), as similar-size bands were obtained for WT and Mut constructs. E, empty vector; M, 1Kb+ DNA marker (Invitrogen); Un, untransfected cells. (*B*) Schematic overview of the genomic region of *LRBA* with *MAB21L2* as a nested pair (located in intron 42 of *LRBA*), and their respective positions in the human genome (hg19). The variant in exon 20 of *LRBA* is located 288.6 Kb away from the start site of *MAB21L2*. (*C*) Immunohistochemistry performed with an HuC/Elavl3 antibody in control and *mab21l2* mutant zebrafish embryos, showed that the absence of *mab21l2* leads to an overall reduction in the numbers of enteric neurons, and aganglionosis is detected in the gut. (*D*) Luciferase assays performed to evaluate a possible enhancer effect of the LRBA variant (c.2444A>G) showed that although exon 20 has enhancer activity when coupled to an SV40 promoter (SV40-P), no difference in luciferase activity could be detected between LRBA WT and LRBA Mut (c.2444A>G) constructs. SV40-E construct was used as a negative control, and a *RET* intronic enhancer element (RET-WT) was used as a positive control.

differences were noticed. Morphant embryos showed a curved body, small eyes, and no swim bladder (Figure 4*D*). Moreover, a significant decrease in the number of enteric neurons was detected when compared with controls (Figure 4*D*). The number of enteric neurons in *ihh* morphants was 13% ± 1.4% of that seen in controls (n = 23), suggesting that *ihh* is required for normal ENS development in zebrafish.

De Novo Deletion in GDNF Leads to Reduced Levels of Secreted Protein and Results in Impaired RET Activation

A heterozygous de novo in-frame deletion in *GDNF* was identified in patient V-4 (NM_001190468.1:c.676–681delG-GATGT). Because this deletion affects 6 base pairs (bp) located just before the last codon of *GDNF*, a change in RNA

stability is expected based on the RNAfold online software (http://rna.tbi.univie.ac.at/cgibin/RNAfold.cgi; Supplementary Figure 2 and Supplementary Table 5). To evaluate this effect, we performed qreal time-PCR on RNA isolated from HEK293 cells transfected with GDNF-WT-Myc-DDK and GDNF-Mut-Myc-DDK–expressing constructs. No significant effect on the mRNA levels was observed in the presence of the deletion (Figure 5*A*). To determine if the in-frame deletion identified impairs the function of GDNF, HEK293 cells transiently expressing RET and GFR-α1, were treated with conditioned medium containing GDNF-WT-Myc-DDK and GDNF-Mut-Myc-DDK. We observed that in the presence of the mutant protein, a decrease in RET expression and phosphorylation levels was observed when compared with the WT. This suggests that the deletion identified does affect the ability of GDNF to activate RET (Figure 5*B*). Moreover, we observed that the GDNF-Mut protein was
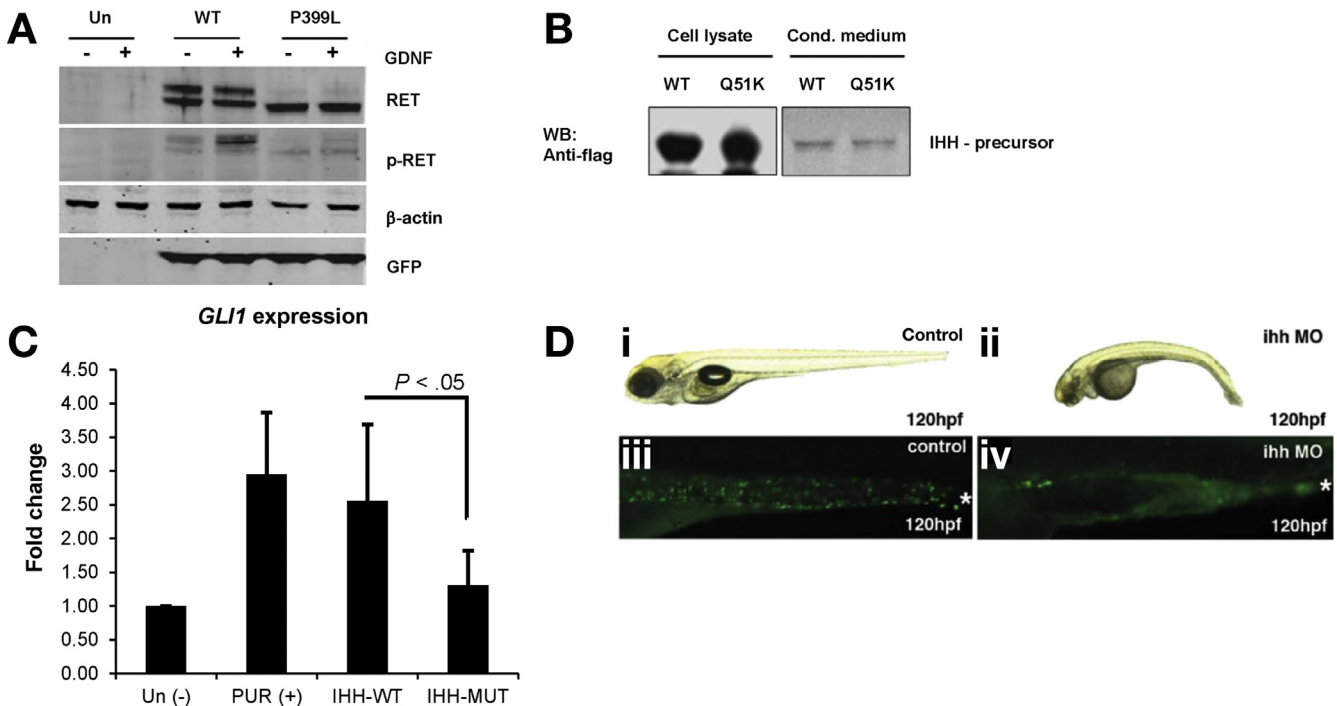
Figure 4. Variants in *RET* and *IHH* have a pathogenic nature. (*A*) Western blot analysis of HEK293 cells transiently expressing pCMV-RET-WT and pCMV-RET-Mut showed that the RET variant identified (c. 1196C>T, p.RET-P399L), leads to a reduction of glycosylated protein, as well as a reduction in the levels of phosphorylated RET. β-actin was used as loading control and GFP as transfecting control. (+) presence and (−) absence of GDNF (50 ng/mL). UT, untransfected. (*B*) Western blot analysis of HEK293 cells transiently expressing IHH-WT-FLAG and IHH-Q51K-FLAG showed no difference in the expression of IHH precursor (~46 kDa). (*C*) qreal time-PCR performed in fibroblasts grown in the presence of conditioned medium containing IHH-WT or IHH-Q51K secreted proteins, showed that cells stimulated with the mutant IHH have reduced expression of *GLI1* when compared with cells stimulated with the WT protein. Purmorphamine (PUR+), an activator of the Hh signaling, was used as a positive control. (*D*) Analysis of the uninjected control and *ihh* morphant embryos at 120 hpf showed that the absence of *ihh* led to curvature of the body, smaller eyes, craniofacial abnormalities, and a loss of swim bladder. Moreover, a decreased number of enteric neurons was observed in morphant embryos after staining with an Elavl3-specific antibody. * marks the anus of the fish.

absent in the conditioned medium (~30 kDa), but it was still present inside the cells. The opposite situation was detected for GDNF-WT (Figure 5*C*). Based on our results, we concluded that the 6-bp deletion impairs secretion of GDNF, thus resulting in less RET activation.

Discussion

A complete understanding of the genetics of an inherited complex disease is a major challenge requiring substantial efforts. In this study, we used a combination of whole-exome sequencing and functional assays to find the underlying causes of HSCR in a multigenerational Dutch family.

Multiple Variants Contribute to HSCR

Finding multiple contributing variants seems logical for a disease with reduced penetrance, such as HSCR. Therefore, we were not surprised to find that 4 different genes appear to modulate disease expression in this family. In the first branch, a missense variant in *RET* was identified (Figure 1). This variant (c.1196C>T, p.P399L), was predicted to affect the extracellular domain of RET and result

in RET dysfunction. Our in vitro studies confirmed this prediction, and showed that the variant identified was pathogenic, as it affected glycosylation and phosphorylation of RET (Figure 4*A*). A previous study of this family also reported that all 3 affected siblings (V-1, V-2, and V-3) inherited a common heterozygous *RET* risk haplotype from their father (IV-1).[18] This haplotype is located in intron 1 of *RET* and has been shown to increase susceptibility for HSCR[36] by affecting *RET* expression.[33,37] Considering that the mother (IV-2) does not have HSCR despite carrying the pathogenic *RET* variant (c.1196C>T, p.P399L), it is logical to consider that the presence of the risk haplotype enhanced the penetrance of the *RET* variant, contributing to the development of the disease in patients V-1, V-2, and V-3.

In the second branch of this family, 2 missense variants located in *IHH* (NM_002181.3:c.151C>A) and *GLI3* (NM_000168.5:c.2119C>T; p.P707S), and 1 de novo deletion in *GDNF* (c.676–681delGGATGT), have been found to underlie HSCR pathogenesis in patient V-4 (Figure 1). *IHH* and *GLI3* encode members of the Hh pathway, whereas *GDNF* encodes a RET ligand. Hh signaling is known to be essential for the development of a variety of tissues and
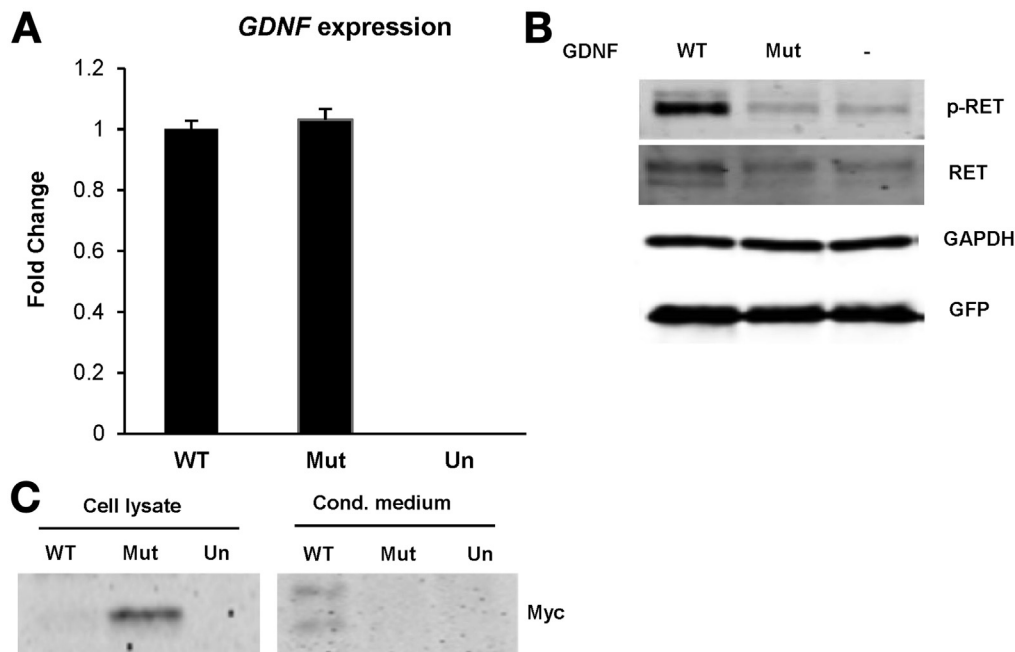
Figure 5. De novo deletion in GDNF affects protein secretion and RET activation. (*A*) qreal time-PCR performed using RNA isolated from HEK293 cells transfected with GDNF-WT and GDNF-Mut constructs, shows that the 6-bp deletion identified has no effect on the levels of RNA present. (*B*) Western blot performed in HEK293 cells transiently expressing RET-WT, GFR-α1, and GFP, and grown in conditioned medium containing GDNF-WT and GDNF-Mut, showed that cells stimulated with the mutant GDNF have reduced levels of phosphorylated RET when compared with cells stimulated with the WT protein. Conditioned medium collected from untransfected HEK293 cells was used as negative control. Glyceraldehyde 3-phosphate dehydrogenase (GAPDH) was used as loading control and GFP as transfecting control. (*B*) Western blot analysis of HEK293 cells transiently expressing GDNF-WT-Myc and GDNF-Mut-Myc showed impaired secretion of the mutant protein ($\sim$30 kDa). $-$, absence of GDNF.

organs and is required for normal ENS development in zebrafish.[38] Despite a previous suspicion of the involvement of *IHH* in HSCR,[39] the Hh signaling was only recently linked to this disease, when mutations in the *GLI* family of transcription factors, known as effectors of Hh signaling, were found in a series of patients with HSCR.[40] Our functional studies support this involvement, as they confirmed the pathogenic nature of the *IHH* variant identified (Figure 4*C*), and showed that the absence of *ihh* in zebrafish leads to an HSCR-like phenotype (Figure 4*D*). The same effect has been previously observed in mice. However, only 50% of *Ihh* knockout mice showed aganglionosis, suggesting that depletion of this gene is not fully penetrant, and disruption of additional genes is required for the intestinal phenotype observed.[41] To date, it is still unclear how IHH affects ENS development, and further studies are required to determine if intestinal aganglionosis is due to a failure of migration of enteric neural crest cells from the vagal neural crest region into and along the gut tube, or whether IHH is required for proliferation of enteric neural crest cells once they enter the gastrointestinal tract. For *GLI3*, we found that the variant identified in patient V-4 and her father (c.2119C>T; p.P707S) has also been reported in patients with Greig cephalopolysyndactyly syndrome (MIM 175700), a rare disorder characterized by craniofacial abnormalities, polydactyly, and syndactyly of hands and feet.[42] Previous studies have shown that this variant is pathogenic, as it leads to abnormal subcellular localization of GLI3 and reduced

transcriptional activity.[43] However, neither IV-4 nor V-4 have any of the features seen in patients with Greig cephalopolysyndactyly syndrome,[18,44] leading us to conclude that this is a low-penetrance variant, likely requiring additional factors to modulate disease expression. Finally, a de novo variant in *GDNF* was also identified comprising an inframe 6-bp deletion that led to the loss of 2 amino acids (c.676–681delGGATGT). Our results showed that this deletion has a pathogenic effect, as it impairs GDNF secretion and leads to reduced RET activation (Figure 5*B* and 5*C*). Mutations in *GDNF* have been previously reported in a few HSCR cases.[20,21] However, it has been postulated that they are not sufficient to cause HSCR on their own, and require additional contributing factors.[20,21,45] In this particular case, we hypothesize that the variants identified in *IHH* and *GLI3* are these additional factors, especially because they are found in a heterozygote state in this family. Previously, we have proposed a model for disturbed ENS development, in which harmful and protective factors balance on a fulcrum representing a disease-specific genetic predisposition.[14] In this model, mild variants that are harmless by themselves can lead to a disease phenotype if found together. For patient V-4, we believe that the deletion in *GDNF* is the one predisposing for HSCR, as it is the only variant present exclusively in patient V-4 and not in her healthy father (IV-4). However, it is the additive effect of the variants identified in *IHH* and *GLI3* that triggers HSCR development in this patient.

LRBA and MAB21L2

Based on the previously performed linkage analysis,[18] we were expecting to find the causative gene for HSCR in this family on chromosome 4. Therefore, we initially focused our efforts on LRBA, as this was the only gene in the linkage region that showed expression in mouse gut.[34] Our functional studies failed to confirm a direct involvement of LRBA in HSCR pathogenesis, and could not support a direct role for lrba in ENS development in zebrafish (Figures 2 and 3). Within LRBA, another gene can be found, MAB21L2, specifically located in intron 42 of LRBA. MAB21L2 is known to play a role in neural development, and here we show that this gene is required for ENS development in zebrafish (Figure 3C). Based on this evidence, MAB21L2 was considered to be a possible candidate gene for HSCR in this family, but because we could not identify any pathogenic variant in this gene in any of the affected members, and failed to show an effect of the LRBA variant identified on MAB21L2 expression, we were unable to link MAB21L2 to HSCR. Therefore, although we believe that MAB21L2 could play a role in HSCR pathogenesis

based on its function, the risk allele on chromosome 4 for this family cannot be attributed to MAB21L2 or LRBA, and remains to be identified.

Consequences for Genetic Counseling

Complex inheritance in families with variable expression and incomplete penetrance is to be expected in HSCR. However, searching for multiple variants that in concert can explain disease variation and penetrance within such families is rare. Common practice in diagnostic laboratories is to search for mutations in the major known disease-associated gene. For HSCR, this means screening the RET gene. If a mutation is identified, the search for additional causing genes stops. However, in some families, this may not represent the full genetic etiology of the disease, leading to a miscalculation of the real genetic risk. Using the family described in this study as an example, the extensive genetic analysis was performed only because the RET variant (c.1196C>T, p.P399L) was missed in the initial screening.[46] One could argue that for the branch in which this variant was found, the additional screen hardly
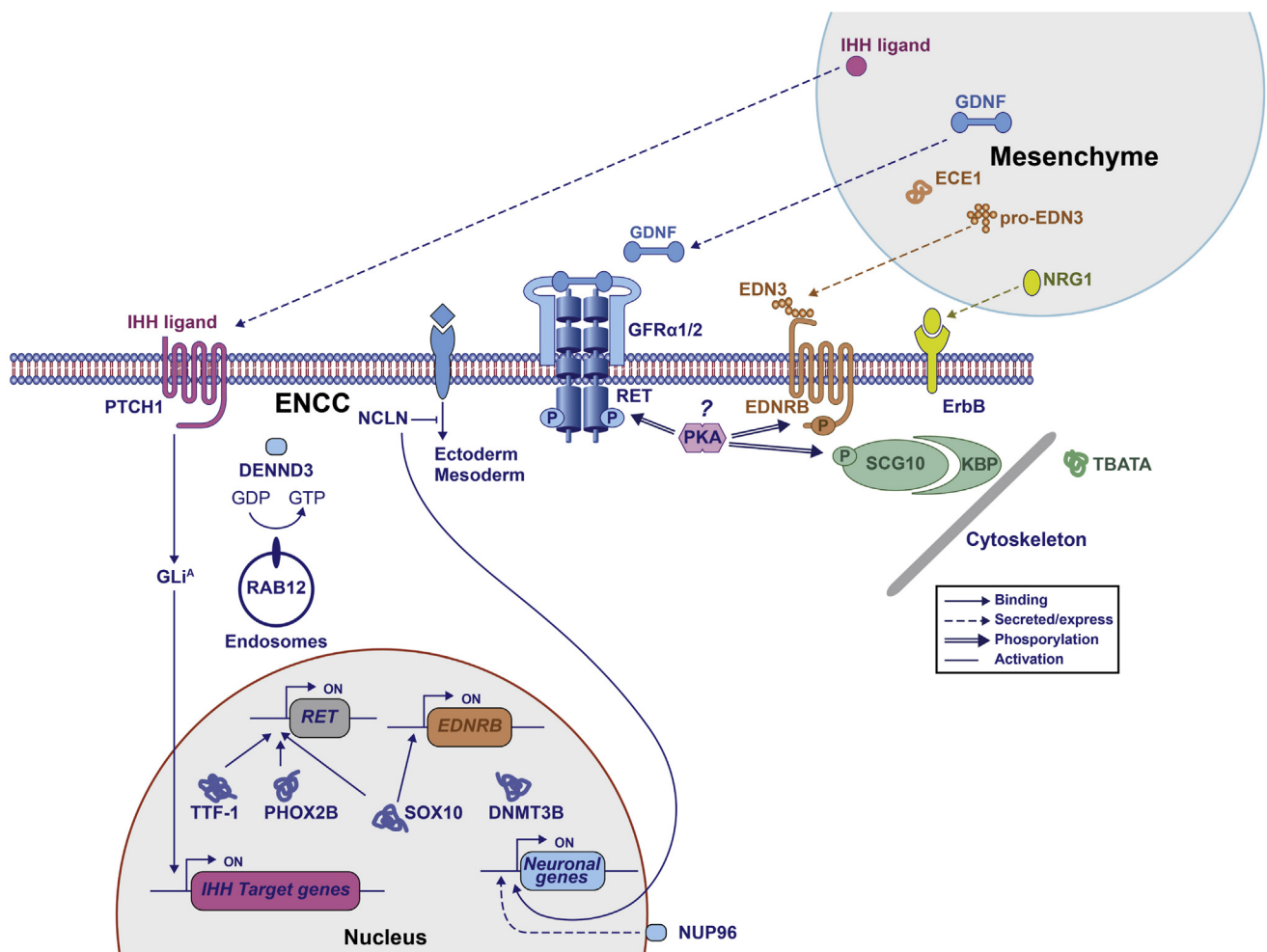

Figure 6. Schematic representation of the known and the newly identified HSCR genes.

adds any useful information, as *RET* probably determines most of the penetrance. However, in the *RET* negative branch, the additional genetic screening proved to be necessary. Finding a de novo *GDNF* deletion, in combination with 2 inherited variants in members of the Hh pathway (*IHH* and *GLI3*), changed genetic counseling, as we now predict a low recurrence risk for this branch of the family. Based on our findings, we believe that an extensive genetic screen can change genetic counseling of a complex genetic disease, especially if a de novo search is added. However, one should be cautious to counsel based only on the presence of a de novo variant, because it is difficult to assess the contribution of such variants to the overall disease risk.

Conclusions

HSCR is a complex disorder in which several genes are known to play a role (Figure 6). Although in 20% of the cases the genetic cause relies on the presence of a single deleterious mutation in a specific gene,[45] for most patients it is likely that rare mutations affecting more than 1 gene are involved in disease pathogenesis. In this study, we report such a family, in which mutations in members of the major disease-associated pathway, *RET* and *GDNF*, in combination with mutations in *GLI3* and in a previously unrelated HSCR gene, *IHH*, are likely to modulate the clinical expression of the disease phenotype (Figure 6). In addition, our results show that even familial cases can have a high genetic complexity, something that should be taken into account when counseling and performing genetic tests for disorders with a presumed multifactorial etiology.

Supplementary Material

Note: To access the supplementary material accompanying this article, visit the online version of *Gastroenterology* at www.gastrojournal.org, and at https://doi.org/10.1053/j.gastro.2018.03.034.

References

1. Heanue TA, Pachnis V. Enteric nervous system development and Hirschsprung's disease: advances in genetic and stem cell studies. Nat Rev Neurosci 2007; 8:466–479.
2. Badner JA, Sieber WK, Garver KL, et al. A genetic study of Hirschsprung disease. Am J Hum Genet 1990;46:568–580.
3. Alves MM, Sribudiani Y, Brouwer RW, et al. Contribution of rare and common variants determine complex diseases-Hirschsprung disease as a model. Dev Biol 2013;382:320–329.
4. **Gui H, Schriemer D, Cheng WW**, et al. Whole exome sequencing coupled with unbiased functional analysis reveals new Hirschsprung disease genes. Genome Biol 2017;18:48.
5. **Jiang Q, Arnold S, Heanue T**, et al. Functional loss of semaphorin 3C and/or semaphorin 3D and their epistatic interaction with ret are critical to Hirschsprung disease liability. Am J Hum Genet 2015;96:581–596.
6. Edery P, Lyonnet S, Mulligan LM, et al. Mutations of the RET proto-oncogene in Hirschsprung's disease. Nature 1994a;367:378–380.
7. Angrist M, Kauffman E, Slaugenhaupt SA, et al. A gene for Hirschsprung disease (megacolon) in the pericentromeric region of human chromosome 10. Nat Genet 1993; 4:351–356.
8. Edery P, Pelet A, Mulligan LM, et al. Long segment and short segment familial Hirschsprung's disease: variable clinical expression at the RET locus. J Med Genet 1994; 31:602–606.
9. Lyonnet S, Bolino A, Pelet A, et al. A gene for Hirschsprung disease maps to the proximal long arm of chromosome 10. Nat Genet 1993;4:346–350.
10. Romeo G, Ronchetto P, Luo Y, et al. Point mutations affecting the tyrosine kinase domain of the RET proto-oncogene in Hirschsprung's disease. Nature 1994; 367:377–378.
11. Burzynski GM, Nolte IM, Osinga J, et al. Localizing a putative mutation as the major contributor to the development of sporadic Hirschsprung disease to the RET genomic sequence between the promoter region and exon 2. Eur J Hum Genet 2004;12:604–612.
12. **Emison ES, McCallion AS**, Kashuk CS, et al. A common sex-dependent mutation in a RET enhancer underlies Hirschsprung disease risk. Nature 2005; 434:857–863.
13. Attie T, Pelet A, Edery P, et al. Diversity of RET proto-oncogene mutations in familial and sporadic Hirschsprung disease. Hum Mol Genet 1995;4:1381–1386.
14. Brosens E, Burns AJ, Brooks AS, et al. Genetics of enteric neuropathies. Dev Biol 2016;417:198–208.
15. Bolk S, Pelet A, Hofstra RM, et al. A human model for multigenic inheritance: phenotypic expression in Hirschsprung disease requires both the RET gene and a new 9q31 locus. Proc Natl Acad Sci U S A 2000;97:268–273.
16. **Gabriel SB, Salomon R**, Pelet A, et al. Segregation at three loci explains familial and population risk in Hirschsprung disease. Nat Genet 2002:3189–3193.
17. Carrasquillo MM, McCallion AS, Puffenberger EG, et al. Genome-wide association study and mouse model identify interaction between RET and EDNRB pathways in Hirschsprung disease. Nat Genet 2002; 32:237–244.
18. **Brooks AS, Leegwater PA**, Burzynski GM, et al. A novel susceptibility locus for Hirschsprung's disease maps to 4q31.3-q32.3. J Med Genet 2006;43:e35.
19. **Garcia-Barcelo MM, Tang CS**, Ngan ES, et al. Genome-wide association study identifies NRG1 as a susceptibility locus for Hirschsprung's disease. Proc Natl Acad Sci U S A 2009;106:2694–2699.
20. Angrist M, Bolk S, Halushka M, et al. Germline mutations in glial cell line-derived neurotrophic factor (GDNF) and RET in a Hirschsprung disease patient. Nat Genet 1996; 14:341–344.
21. Salomon R, Attie T, Pelet A, et al. Germline mutations of the RET ligand GDNF are not sufficient to cause Hirschsprung disease. Nat Genet 1996;14:345–347.

22. Doray B, Salomon R, Amiel J, et al. Mutation of the RET ligand, neurturin, supports multigenic inheritance in Hirschsprung disease. Human Mol Genet 1998; 7:1449–1452.

23. Miller SA, Dykes DD, Polesky HF. A simple salting out procedure for extracting DNA from human nucleated cells. Nucleic Acids Res 1988;16:1215.

24. Widowati T, Melhem S, Patria SY, et al. RET and EDNRB mutation screening in patients with Hirschsprung disease: functional studies and its implications for genetic counseling. Eur J Hum Genet 2016;24:823–829.

25. Kennedy BN, Stearns GW, Smyth VA, et al. Zebrafish rx3 and mab21l2 are required during eye morphogenesis. Dev Biol 2004;270:336–349.

26. Hartsock A, Lee C, Arnold V, et al. In vivo analysis of hyaloid vasculature morphogenesis in zebrafish: a role for the lens in maturation and maintenance of the hyaloid. Dev Biol 2014;394:327–339.

27. **Korzh S, Winata CL**, Zheng W, et al. The interaction of epithelial Ihha and mesenchymal Fgf10 in zebrafish esophageal and swimbladder development. Dev Biol 2011;359:262–276.

28. Shepherd IT, Pietsch J, Elworthy S, et al. Roles for GFRalpha1 receptors in zebrafish enteric nervous system development. Development 2004;131:241–249.

29. Robu ME, Larson JD, Nasevicius A. p53 activation by knockdown technologies. PLoS Genet 2007;3:e78.

30. Halim D, Hofstra RM, Signorile L, et al. ACTG2 variants impair actin polymerization in sporadic megacystis microcolon intestinal hypoperistalsis syndrome. Hum Mol Genet 2016;25:571–583.

31. Van Der Werf CS, Wabbersen TD, Hsiao NH, et al. CLMP is required for intestinal development, and loss-of-function mutations cause congenital short-bowel syndrome. Gastroenterology 2012;142:453–462.

32. Alves MM, Halim D, Maroofian R, et al. Genetic screening of congenital short bowel syndrome patients confirms CLMP as the major gene involved in the recessive form of this disorder. Eur J Hum Genet 2016;24:1627–1629.

33. Sribudiani Y, Metzger M, Osinga J, et al. Variants in RET associated with Hirschsprung's disease affect binding of transcription factors and gene expression. Gastroenterology 2011;140:572–582.e572.

34. Schriemer D, Sribudiani Y, IJpma A, et al. Regulators of gene expression in Enteric Neural Crest Cells are putative Hirschsprung disease genes. Dev Biol 2016; 416:255–265.

35. Tsang WH, Shek KF, Lee TY, et al. An evolutionarily conserved nested gene pair - Mab21 and Lrba/Nbea in metazoan. Genomics 2009;94:177–187.

36. Burzynski GM, Nolte IM, Bronda A, et al. Identifying candidate Hirschsprung disease-associated RET variants. Am J Hum Genet 2005;76:850–858.

37. Emison ES, Garcia-Barcelo M, Grice EA, et al. Differential contributions of rare and common, coding and non-coding Ret mutations to multifactorial Hirschsprung disease liability. Am J Hum Genet 2010;87:60–74.

38. Reichenbach B, Delalande JM, Kolmogorova E, et al. Endoderm-derived Sonic hedgehog and mesoderm Hand2 expression are required for enteric nervous system development in zebrafish. Dev Biol 2008; 318:52–64.

39. **Garcia-Barceló MM, Lee WS**, Sham MH, et al. Is there a role for the IHH gene in Hirschsprung's disease? Neurogastroenterol Motil 2003;15:663–668.

40. Liu JA, Lai FP, Gui HS, et al. Identification of GLI mutations in patients with Hirschsprung disease that disrupt enteric nervous system development in mice. Gastroenterology 2015;149:1837–1848.

41. Ramalho-Santos M, Melton DA, McMahon AP. Hedgehog signals regulate multiple aspects of gastrointestinal development. Development 2000;127:2763–2772.

42. Wild A, Kalff-Suske M, Vortkamp A, et al. Point mutations in human GLI3 cause Greig syndrome. Hum Mol Genet 1997;6:1979–1984.

43. Krauss S, So J, Hambrock M, et al. Point mutations in GLI3 lead to misregulation of its subcellular localization. PLoS One 2009;4:e7471.

44. Biesecker LG. Pallister-Hall syndrome. 1993.

45. Amiel J, Sproat-Emison E, Garcia-Barcelo M, et al. Hirschsprung disease, associated syndromes and genetics: a review. J Med Genet 2008;45:1–14.

46. Hofstra RM, Wu Y, Stulp RP, et al. RET and GDNF gene scanning in Hirschsprung patients using two dual denaturing gel systems. Hum Mutat 2000;15:418–429.

BASIC AND TRANSLATIONAL AT

Supplementary Material and Methods

Exome Sequencing and Variant Prioritization

Three micrograms of DNA from each of the individuals was sheared using acoustic technology (Covaris, Inc, Woburn, MA). Target enrichment for V-1 and V-4 was performed with the SureSelect Human All Exon 50 Mb Targeted exome enrichment kit v4, and for the trio (IV-4, IV-5, and V-4) the Agilent Sureselect CRE capture kit (Agilent Technologies, Inc, Santa Clara, CA) was used. Captured fragments were sequenced (paired-end 101-bp read length) on the Illumina HiSeq2000 (Sureselect V4) and HiSeq2500 (CRE) sequencers (Illumina, San Diego, CA). De-multiplexing, alignment to the human genome build 19 (Hg19) reference genome, and curation of low-quality reads were done as described by our in-house developed NARWHAL pipeline.[1] BAM-files were generated with SAMtools version 0.1.12a,[2] and variant calling was performed with the Bayesian genotyper incorporated in the genome analysis toolkit version 1.2.9.[3] Variant files generated of VCFv4 format were uploaded into Cartagenia Bench NGS version 5.0 (Cartagenia Inc, Boston, MA) for filtering with previously described settings.[4]

Vector Design and Site Direct Mutagenesis

The genomic region of *LRBA* containing exon 20 and its flanking sequence (approximately 400 bp), was amplified from control and patient DNA to obtain WT and Mut (NM_001199282.2:*c*.2444A>G) alleles, respectively, using primers described in Supplementary Table 1 (LRBAF and LRBAR). PCR products obtained, LRBA-Enh-WT and LRBA-Enh-Mut, were inserted into the pCR 2.1-TOPO vector, subsequently digested with *Xho*I and *Kpn*I restriction enzymes, and cloned into a pGL3-SV40 promoter (SV40-P) upstream of the luciferase gene (Promega, Madison, WI), to generate the pGL3-SV40p-Luc-LRBA-Enh-WT and pGL3-SV40p-Luc-LRBA-Enh-Mut vectors. The same LRBA PCR products, LRBA-Enh-WT and LRBA-Enh-Mut, were also directly cloned into the exon trapping vector pSPL3 (Invitrogen, Carlsbad, CA) to generate the pSPL3-LRBA-WT and the pSPL3-LRBA-Mut vectors. The pRc/CMV-RET-WT vector,[5] encoding the short isoform of human RET (RET9), was used to create the pRc/CMV-RET-Mut (P399L) by site-directed mutagenesis, according to the manufacturer's instructions (Stratagene, La Jolla, CA). The pCMV-IHH-FLAG-WT vector[6] and pCMV6-Entry-GDNF-Myc-DDK vector (Origene, Rockville, MD) were used to create pCMV-IHH-FLAG-Mut (Q51K) and pCMV6-Entry-GDNF-Mut (Gly226_-Cys227del)-Myc-DDK, respectively, by site-directed mutagenesis, according to the manufacturer's instructions (Stratagene and New England Biolabs, Ipswich, MA). All inserts were Sanger-sequenced to confirm the presence of the WT and Mut variants, as well as the orientation of the inserted fragments. Primers used (RET-MutF; RET-MutR; IHH-MutF, IHH-MutR, GDNF-MutF, and GDNF-MutR) are described in Supplementary Table 1.

## Whole-Mount In Situ Hybridization for lrba, mab21l2, and ihh in Zebrafish

lrba, mab21l2, and *ihh* genes were amplified from total mRNA collected from zebrafish embryos by RT-PCR. Amplified bands were gel-purified and sub-cloned into TOPO TA PCRII vector (Thermo Fisher, Waltham, MA). Digoxigenin-labeled antisense probes (Roche, Basel, Switzerland) were generated using SP6 polymerase (Roche) after linearizing the plasmid templates using *Not*I restriction enzyme (New England Biolabs). Embryos were collected and processed for whole-mount in situ hybridization as previously described.[7] Digoxigenin-labeled probes were visualized with NBT/BCIP coloration reactions.

RNA Isolation and qReal time-PCR

RNA isolation was performed with the RNeasy mini kit (Qiagen, Valencia, CA) according to the manufacturer's instructions. cDNA preparation was done with the iScrip cDNA synthesis kit (Bio-Rad, Hercules, CA), using 1 µg RNA isolated from fibroblasts treated with Purmophamine and conditioned medium containing IHH-WT and IHH-Mut. *GLI1* expression levels were determined by quantitative real-time (qreal-time) Sybr Green PCR, using the 7300 Real-time PCR platform system (Applied Biosystems, Foster City, CA). The same procedure was used to determine levels of GDNF in HEK293 cells transfected with GDNF-WT and GDNF-Mut vectors. *CLK2* was used as a housekeeping gene to normalize *GLI1* expression levels, while *GAPDH* and *ACTB* were used for *GDNF* (primer details in Supplementary Table 1). qreal time-PCR data were analyzed using a method previously described,[8] and presented as fold changes. These assays were performed in 3 independent triplicates (n = 9).

Supplementary Figure 1. *mab21l2* expression pattern in zebrafish. In situ hybridization showing that *mab21l2* has a strong expression in the hindbrain (*black arrows*) and pharyngeal arches (*white arrows*) through all time points (24–96 hpf). From 48 hpf onward, a strong expression is also detected in the gut mesoderm (*).
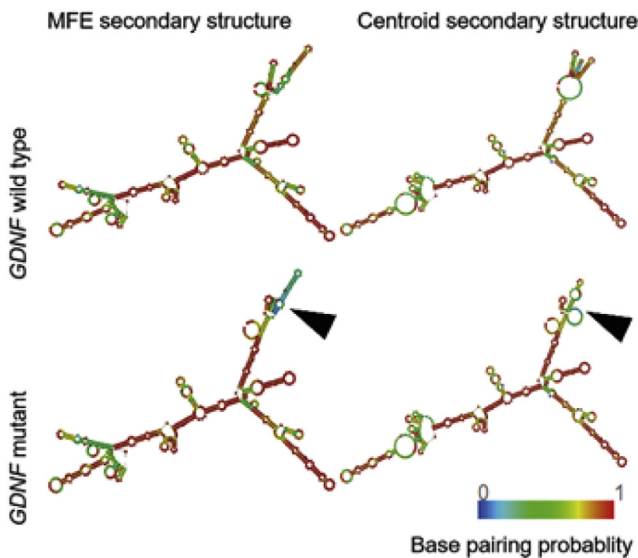
Supplementary Figure 2. A decrease in RNA stability is predicted in the presence of the de novo deletion in *GDNF*, by in silico analysis. Secondary structures of *GDNF* WT and Mut RNA determined using RNAfold software, showed that a change in both the minimum free energy (MFE) and the centroid secondary structures are predicted to occur in the presence of the deletion identified (*arrowheads*). Each color indicates the probability of individual nucleotides to participate in the structure, and range from the highest (*red*) to the lowest probability (*blue-violet*).

Supplementary Table 1. List of Primers Used in This Study

Gene	Primer (5′–3′)
*LRBA*F	CCACATAACTTAAGGTTGATTC
*LRBA*R	GATATAAGGAGATGTGGCTG
*RET*F	CTGGCCAGCCCATCTTGG
*RET*R	CCGAGTCACCATATGCAGATTTACC
*IHH*F	ATCAGCCCACCAGGAGACC
*IHH*R	CATCAGCCCACCAGGAGACC
*GLI3*F	AGTGGCCAGCTCCATTCACC
*GLI3*R	GGTTACAGCGTCATTTTAGGACTGG
*GDNF*F	TTTCAAACCCTAATGCACTTTTATTCC
*GDNF*R	TGACCTGGAAAAGGCCAAGG
RET-MutF	CGTGTCGGTGCTGC**T**GGTCAGCCTGCAC
RET-MutR	GTGCAGGCTGACC**A**GCAGCACCGACACG
IHH-MutF	CGCTCGCCTACAAG**A**AGTTCAGCCCCAATG
IHH-MutR	CATTGGGGGCTGAACT**T**CTTGTAGGCGAGCG
GDNF-MutF	ATCACGCGTACGCGGCCG
GDNF-MutR	ACACCTTTTAGCGGAATGCTTTCTTAGAATATGG
SD6	TCTGAGTCACCTGGACAACC
SA2	ATCTCAGTGGTATTTGTGAGC
*lrba*F	CTTTTGACCAAAGGAATGGGTTACG
*lrba*R	TCCAAGCATGACTTCTGCTTTCC
*ihh*F	GAATTTTACGCACGGACGAT
*ihh*R	CGTAATGCAGCGAATCTTCA
*mab21l2*F	ATTCGCTCCCGCTTTCAG
*mab21l2*R	TCGTCCCAGTCAGTCTCCC
*GLI1*qF	TCCCCATGACTCTGCCCG
*GLI1*qR	CCAGCATGTCCAGCTCAGA
*GDNF*qF	CGCTGAGCAGTGACTCAAAT
*GDNF*qR	AGGAAGCACTGCCATTTGTT
*CLK2*qF	TCGTTAGCACCTTAGGAGAGG
*CLK2*qR	TGATCTTCAGGGCAACTCG
*ACTB*qF	AACCGCGAGAAGATGACCC
*ACTB*qR	GCCAGAGGCGTACAGGGATAG
*GAPDH*qF	CGACCTTCACCTTCCCCAT
*GAPDH*qR	TAAAAGCAGCCCTGGTGACC

Supplementary Table 2. List of Antibodies Used for Western Blot

Antibodies	Host	Dilution
RET	Rabbit	1:1000
p-RET	Rabbit	1:1000
Myc	Mouse	1:1000
β-Actin	Mouse	1:1000
GAPDH	Mouse	1:10,000
GFP	Rabbit	1:2000
Flag	Mouse	1:1000
IRDDye 800	Goat	1:10,000
IRDDye 680	Goat	1:10,000

Supplementary Table 3. In Silico Prediction of the Pathogenic Nature of the Rare Variants Identified in Patients V-1 (a) and V-4 (b)

Sample	Gene	Variant	PHAST score	GERP++ neutral rate	PhyloP score	SiPhy score	Mutation Taster	SIFT score	PolyPhen2 HumVar	LRT prediction	Mutation Assessor	FATHMM score	BLOSUM62	Cadd Phred score
a	*RET*	c.1196C>T	-	5.13	1.151	10.524	1	0	0.856	Deleterious	1.955	−3.02	−3	27.5
a, b	*NRP2*	c.1000C>T	0.9	5.91	1.505	15.056	1	0.02	0.929	Deleterious	2.555	−4.81	−3	35
a, b	*PGRMC2*	c.185G>A	-	3.81	0.927	7.764	0.734	1	0.003	Neutral	−0.345	−1.13	−2	22.6
a, b	*LRBA*	c.2444A>G	1	5.66	0.96	12.981	1	0.01	0.488	Deleterious	2.455	−0.12	1	25.2
a, b	*OR1F1*	c.47G>A	1	4.97	2.456	16.064	0.94	0.01	0.997	Deleterious	3.54	5.95	−2	23.7
a, b	*CLUH*	c.3547G>C	1	5.07	1.248	6.899	0.529	0.08	0.008	Neutral	0.625	−1.58	−1	21.7
a,b	*PELP1*	c.2696T>C	1	4.42	-0.564	0.625	1	64	0	Neutral	1.5	0.92	0	5.925
a,b	*PELP1*	c.2161A>G	1	5.13	-0.013	3.9	1	21	0	Neutral	0.345	0.93	1	0.144
b	*IHH*	c.151C>A	-	4.22	2.18	12.671	1	0	0.965	Deleterious	3.56	−6.03	1	25.2
b	*GLI3*	c.2119C>T	1	5.82	1.468	14.65	1	0.01	0.925	Neutral	2.865	2.18	−1	28.8
b	*GDNF*	c.676_681delGGATGT	-	-	-	-	-	-	-	-	-	-	-	20.5

NOTE. The following thresholds were used to evaluate conservation: PhyloP $\geq$ 0.95; GERP++ $\geq$ 2; SiPhy $\geq$ 5; PHAST conservation score $\geq$ 0; Grantham distance $\geq$ 60. To predict deleteriousness the following thresholds were used: Mutationtaster $\geq$ 0.51; Pph2 hvar $\geq$ 0.909 (complex disease) or Pph2 hdiv $\geq$ 0.956 (Mendelian disease); Mutation assessor $\geq$ 1.91; FATHM $\leq$ -1.50; SIFT $\leq$ 0.049; LRT: deleterious; BLOSUM62 $\leq$ 0; CADD Phred $\geq$ 20 (mutations in the splice interval can have lower values). BLOSUM, Blocks Substitution Matrix; GERP, Genomic Evolutionary Rate Profiling; LRT, likelihood ratio test; PolyPhen, Polymorphism Phenotyping v2.
-, unknown.

Supplementary Table 4. Segregation Analysis of Candidate Variants Identified by Exome Sequencing in the Family Members

Gene	II-2	III-2	IV-1	IV-2	IV-3	IV-4	IV-5	V-1	V-2	V-3	V-4
LRBA (c.2444A>G)	+	+	−	+	+	+	−	+	+	+	+
RET (c.1196C>T)	−	−	−	+	+	−	−	+	+	+	−
IHH (c.151C>A)	−	−	−	−	−	+	−	−	−	−	+
GLI3 (c.2119C>T)	NI	NI	−	−	NI	+	−	−	NI	NI	+

+, present; −, absent; NI, not investigated.

Supplementary Table 5. Differences in Minimum Free Energies and Ensemble Diversity of Predicted Secondary Structures of *GDNF* WT and Mut RNA

	GDNF WT	*GDNF* Mut
Minimum free energy	−192.80 kcal/mol	−18.,40 kcal/mol
Free energy of thermodynamic ensemble	−202.,30 kcal/mol	−197.50 kcal/mol
Ensemble diversity	109.20	100.24
Minimum free energy (centroid secondary structure)	−177.30 kcal/mol	−171.10 kcal/mol

Supplementary References

1. Brouwer RW, van den Hout MC, Grosveld FG, et al. NARWHAL, a primary analysis pipeline for NGS data. Bioinformatics 2012;28:284–285.

2. Li H, Handsaker B, Wysoker A, et al. The Sequence Alignment/Map format and SAMtools. Bioinformatics 2009;25:2078–2079.

3. McKenna A, Hanna M, Banks E, et al. The Genome Analysis Toolkit: a MapReduce framework for analyzing next-generation DNA sequencing data. Genome Res 2010;20:1297–1303.

4. Halim D, Brosens E, Muller F, et al. Loss-of-function variants in MYLK cause recessive megacystis micro-colon intestinal hypoperistalsis syndrome. Am J Hum Genet 2017;101:123–129.

5. Plaza Menacho I, Koster R, van der Sloot AM, et al. RET-familial medullary thyroid carcinoma mutants Y791F and S891A activate a Src/JAK/STAT3 pathway, independent of glial cell line-derived neurotrophic factor. Cancer Res 2005;65:1729–1737.

6. Ma G, Yu J, Xiao Y, et al. Indian hedgehog mutations causing brachydactyly type A1 impair Hedgehog signal transduction at multiple levels. Cell Res 2011;21:1343–1357.

7. Thisse C, Thisse B. High-resolution in situ hybridization to whole-mount zebrafish embryos. Nat Protoc 2008;3:59–69.

8. Livak KJ, Schmittgen TD. Analysis of relative gene expression data using real-time quantitative PCR and the 2(-Delta Delta C(T)) Method. Methods 2001;25:402–408.